Programmed death-1 (PD-1)–deficient mice are extraordinarily sensitive to tuberculosis

Eszter Lázár-Molnár[a], Bing Chen[a,b], Kari A. Sweeney[a,b], Emilie J. Wang[a], Weijun Liu[a], Juan Lin[c], Steven A. Porcelli[a], Steven C. Almo[d,e], Stanley G. Nathenson[a,f,1], and William R. Jacobs, Jr.[a,b,g,1]

[a]Department of Microbiology and Immunology, [b]Howard Hughes Medical Institute, [c]Departments of Epidemiology and Population Health, [d]Biochemistry, [e]Physiology and Biophysics, [f]Cell Biology, and [g]Molecular Genetics, Albert Einstein College of Medicine, Bronx, NY 10461

Contributed by Stanley G. Nathenson, June 2, 2010 (sent for review March 26, 2010)

The programmed death-1 (PD-1) costimulatory receptor inhibits T and B cell responses and plays a crucial role in peripheral tolerance. PD-1 has recently been shown to inhibit T cell responses during chronic viral infections such as HIV. In this study, we examined the role of PD-1 in infection with *Mycobacterium tuberculosis*, a common co-infection with HIV. PD-1–deficient mice showed dramatically reduced survival compared with wild-type mice. The lungs of the PD-1$^{-/-}$ mice showed uncontrolled bacterial proliferation and focal necrotic areas with predominantly neutrophilic infiltrates, but a lower number of infiltrating T and B cells. Proinflammatory cytokines, such as TNF-α, IL-1, and especially IL-6 and IL-17 were significantly increased in the lung and sera of infected PD-1$^{-/-}$ mice, consistent with an aberrant inflammation. Microarray analysis of the lungs infected with *M. tuberculosis* showed dramatic differences between PD-1$^{-/-}$ and control mice. Using high-stringency analysis criteria (changes of twofold or greater), 367 transcripts of genes were differentially expressed between infected PD-1$^{-/-}$ and wild-type mice, resulting in profoundly altered inflammatory responses with implications for both innate and adaptive immunity. Overall, our studies show that the PD-1 pathway is required to control excessive inflammatory responses after *M. tuberculosis* infection in the lungs.

co-inhibitory | costimulatory | infection

Immunosuppression due to the loss of CD4$^+$ T cells, such as occurring in HIV disease, is a major contributing factor in the threatening increase in tuberculosis (TB) (1), which underlies the importance of the adaptive immune response and CD4$^+$ T cells in particular in controlling *Mycobacterium tuberculosis* infection. A better understanding of the way that T cells interact with infected macrophages is essential for the development of new therapies (2, 3). Interactions between T cells and macrophages are regulated by a variety of signals provided by costimulatory molecules, including members of the CD28/B7 family, such as CD28, CTLA4, ICOS, and PD-1, and their various B7 ligands (4). Programmed cell death-1 (PD-1) inhibits T and B cell activation when it binds to one of its two ligands, PD-1 ligand 1 (PD-L1, also called B7-H1) (5), or PD-1 ligand 2 (PD-L2 or B7-DC) (6), in the context of antigen presentation.

Mounting evidence suggests that the inhibitory PD-L/PD-1 pathway plays a central role in the interaction between host and pathogenic microbes (7). A number of pathogens were shown to induce immune evasion by up-regulating PD-1 or its ligands, and in all of these models, blockade of the PD-L/PD-1 pathway enhanced immune functions for the benefit of the host. For example in chronic viral infections such as lymphocytic choriomeningitis virus (LCMV) in mice (8) and HIV in humans (9), functional impairment (exhaustion) of virus-specific CD8$^+$ T cells has been associated with elevated PD-1 expression on the exhausted cells. Blockade of the PD-1/PD-L pathway reverses the exhaustion of virus-specific T cells and restores effector functions, cytokine production, and cell proliferation. Parasites such as *Schistosoma mansoni* and *Taenia crassiceps* have been shown to suppress effective immune responses by up-regulating PD-1 ligands on host macrophages, which, in turn, inhibit activated T cells (10, 11). Moreover, studies by our group have shown that the PD-1 pathway regulates susceptibility to the macrophage resident fungal respiratory pathogen *Histoplasma capsulatum.* By using a mouse model of histoplasmosis, all PD-1$^{-/-}$ mice cleared the fungus and survived, while control mice succumbed to the lethal dose. Notably, antibody blockade of PD-1 significantly increased survival (70%) of lethally infected wild-type mice, suggesting a potential novel strategy of immunotherapy for histoplasmosis (12).

In this study, we examined the hypothesis that the PD-1–deficient mice will elicit efficient sterilizing immune response against virulent *M. tuberculosis*. To test this hypothesis, we infected PD-1$^{-/-}$ mice via aerosol challenge. Surprisingly, PD-1–deficient mice were extremely sensitive to *M. tuberculosis* aerosol infection, showing dramatically reduced survival and higher bacterial loads. This was associated with profoundly up-regulated inflammatory responses in the lungs, with implications in both innate and adaptive immunity. Our data demonstrate that the PD-L/PD-1 pathway plays a paradoxical but critical role in regulating host responses after virulent *M. tuberculosis* infection in the lung, and may help to guide development of immunotherapies involving manipulation of this pathway.

Results

Dramatically Reduced Survival of PD-1–Deficient Mice After Aerosol Infection with *M. tuberculosis*. To study the role of PD-1 in virulent tuberculosis, PD-1–deficient and control C57BL/6 mice were compared using an aerosol infection model. Survival and bacterial growth in lungs, liver, and spleen were monitored at various timepoints postinfection. Strikingly, PD-1–deficient mice showed reduced ability to control *M. tuberculosis* H37Rv aerosol infection (Fig. 1). After infection with 320 CFU/mouse, PD-1$^{-/-}$ mice started to succumb as early as 28 d postinfection and were all dead by day 39 postinfection (median survival time 31.5 d). At the lowest dose of infection, 50 CFU/mouse, the survival of PD-1$^{-/-}$ mice was also severely impaired; the median survival time was 137 d. All of the control C57BL/6 mice survived for the entire follow-up period (200 d).

Analysis of bacterial counts after aerosol infection showed significant differences between the lungs of PD-1$^{-/-}$ and wild-type mice (Fig. 2). At 4 wk postinfection, PD-1–deficient mice infected with low-dose aerosol (50 CFU/mouse) had 10-fold higher CFUs compared with wild-type mice, and this difference persisted at later timepoints (Fig. 2*A*). No significant difference was observed at earlier timepoints, such as 24 h or 2 wk postinfection. At higher dose, such as 320 CFU/mouse, the difference in bacterial loads between PD-1$^{-/-}$ and wild-type lungs was

Author contributions: E.L.-M., B.C., and W.R.J. designed research; E.L.-M., B.C., K.A.S., E.J.W., and W.L. performed research; E.L.-M., B.C., and J.L. analyzed data; and E.L.-M., S.A.P., S.C.A., S.G.N., and W.R.J. wrote the paper.

The authors declare no conflict of interest.

[1]To whom correspondence may be addressed. E-mail: jacobsw@hhmi.org or stanley.nathenson@einstein.yu.edu.

This article contains supporting information online at www.pnas.org/lookup/suppl/doi:10.1073/pnas.1007394107/-/DCSupplemental.

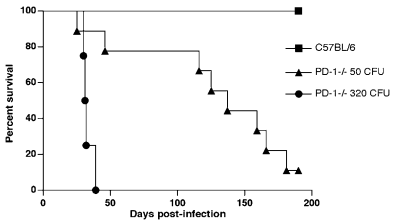

Fig. 1. PD-1–deficient mice show dramatically reduced survival after *M. tuberculosis* H37Rv aerosol infection. PD-1$^{-/-}$ mice are shown as black circles (320 CFU/mouse) or as triangles (50 CFU/mouse). Wild-type mice (squares) survived for >200 d postinfection, after both doses used (320 CFU/mouse shown). Data for 10–15 mice per groups are shown from two independent experiments. Survival curves were compared using log rank test ($P < 0.0001$).

more than 30-fold (Fig. 2*B*). In contrast to the elevated bacterial counts in the lungs of the PD-1$^{-/-}$ mice, no significant differences were found in other target organs examined, such as the liver or spleen (Fig. 2*B* and Fig. S1).

Severe Necrotic Pneumonia Develops in the Lungs of PD-1$^{-/-}$ Mice Infected with *M. tuberculosis*. Histological analysis of the lungs infected with *M. tuberculosis* H37Rv showed extensive focal necrotic areas in the lungs of PD-1–deficient mice (Fig. 3*A*), whereas control mice had fewer and less extensive inflammatory lesions. At 2 wk postinfection both PD-1$^{-/-}$ and wild-type mice had very rare inflammatory nodules (Fig. S2). However, at 4 wk postinfection, both groups developed coalescing nodular pneumonia, but the nature of the inflammation was notably different. Wild-type mice had widespread but moderate granulomatous multifocal pneumonia, and the nodular aggregates were largely histiocytic with infiltrating lymphocytes, with only limited necrosis. In contrast, PD-1$^{-/-}$ mice had necrotizing pneumonia, with large numbers of degenerating and fragmented neutrophils, but no significant lymphocytic infiltrates. The infiltration of neutrophils admixed with degenerating macrophages was associated with extensive necrosis (Fig. 3*B Top*). Nodules appeared to arise surrounding bronchioles, and many bronchioles were packed with or contained scattered neutrophils and nuclear and cellular debris, without significant degeneration of the respiratory epithelium. The centers of these nodules had extensive necrosis of pulmonary parenchyma with loss of architecture, which was replaced by nuclear and cellular debris.

Consistent with the CFU data, acid-fast bacilli (AFB) staining of the lungs showed massive numbers of *M. tuberculosis* organisms throughout the nodules in the lungs of the PD-1–deficient mice (Fig. 3*B Lower*). In contrast to the control mice, which had only limited numbers of acid-fast bacilli located mostly in macrophages within the nodules, the PD-1$^{-/-}$ mice had acid-fast positive mycobacteria localized throughout the lungs, as well as

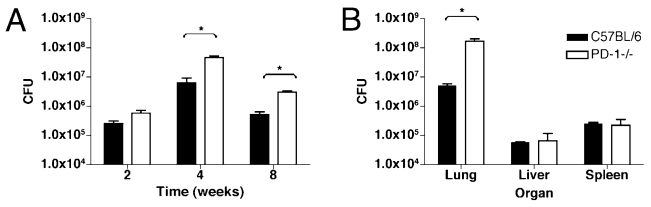

Fig. 2. PD-1–deficient mice have increased bacterial loads in the lungs after H37Rv aerosol infection, compared with wild-type mice. (*A*) cfu values determined in the lungs of wild-type and PD-1$^{-/-}$ mice, 2, 4, and 8 wk after low-dose H37Rv aerosol infection (50 CFU). Mean values of five mice at each timepoint are shown ± SD. (*B*) CFU values from organs of control and PD-1$^{-/-}$ mice at 4 wk postinfection with 320 CFU. Data are representative of three independent experiments. *$P < 0.05$.

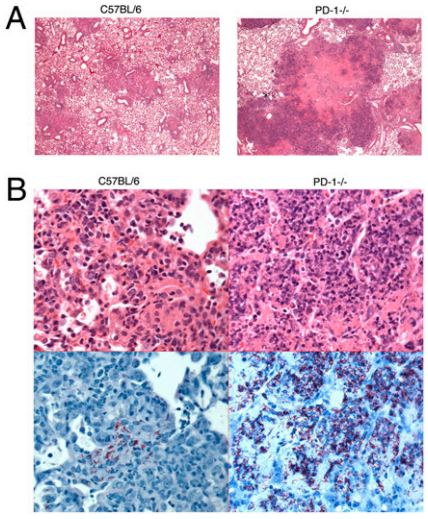

Fig. 3. Histology of the lungs of PD-1$^{-/-}$ and control mice at 4 weeks postinfection with *M. tuberculosis* H37Rv aerosol. (*A*) Lungs of the PD-1$^{-/-}$ mice develop large focal necrotic areas. HE stain at 40× magnification. (*B Upper*) Necrotizing inflammation and neutrophilic infiltration in the lungs of PD-1$^{-/-}$ mice (HE stain at 400× magnification). (*B Lower*) Scattered bacteria in the lungs of C57BL/6 mice (*Left*); massive bacterial load in the lungs of PD-1$^{-/-}$ mice (*Right*), visualized by AFB stain (400×, bacteria are shown in red). Mice were infected with 320 CFU/mouse.

in macrophages in the alveoli, reaching particularly high densities within the necrotic lesions (Fig. 3*B Lower*).

Immunohistochemical staining of the lungs showed a clustered presence of B cells in the lungs of PD-1$^{-/-}$ mice, forming aggregates mostly around airways and vessels; however, in contrast to control mice, B cells were absent from the pyogranulomatous nodules in the lungs of PD-1$^{-/-}$ mice (Fig. S3 *Left*). T cell distribution showed a similar pattern in PD-1$^{-/-}$ and wild-type mice, predominantly around vessels and airways. However, in contrast to wild-type mice, which had numerous T cells in their histiocytic nodules, PD-1$^{-/-}$ mice had only a few T cells infiltrating the pyogranulomatous nodules (Fig. S3 *Right*).

Altered Recruitment of Inflammatory Cells in the Lungs of *M. tuberculosis* Infected PD-1$^{-/-}$ Mice Compared with Wild-Type Mice. To determine whether defective cell recruitment could account for the inability of PD-1$^{-/-}$ mice to control bacterial replication in the lungs, FACS analysis was performed on total lung cells. Reduced total numbers of CD4$^+$ T cells and B cells were found in the lungs of PD-1$^{-/-}$ mice at 4 wk postinfection, whereas CD8$^+$ T cell numbers were similar (Fig. 4 *A–C*). This finding was consistent with the immunohistochemistry data showing very low numbers of B and T cells in the necrotic areas in the PD-1$^{-/-}$ lungs (Fig. S3). Moreover, there was an increase in the CD11b$^+$ (Fig. 4*D*) and Gr1$^+$ cell numbers (Fig. 4*E*) by 3 wk postinfection. These findings indicate that the cellular composition of the infiltrates and kinetics of infiltration differ significantly between the PD-1$^{-/-}$ and wild-type mice, eventually leading to the formation of necrotic pneumonia in the PD-1$^{-/-}$ mice. These data are also consistent with the observed histopathology, showing the predominance of neutrophils and macrophages in the cellular infiltrates in the lungs of infected PD-1$^{-/-}$ mice, in contrast to control mice, which have a more uniform distribution of different cell types, including significant numbers of T and B cells.

Altered Cytokine Responses in *M. tuberculosis*-Infected PD-1$^{-/-}$ Mice. The observed major differences in survival, histopathology, and composition of cellular infiltrates in the lungs of *M. tuberculosis*-infected PD-1$^{-/-}$ versus control mice suggested that markedly

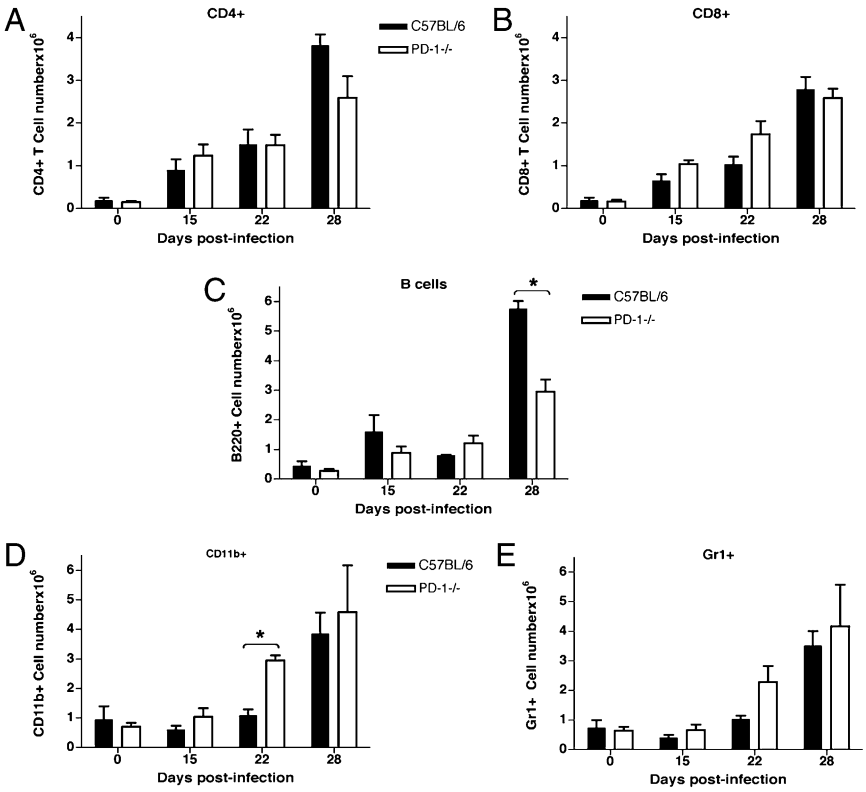

Fig. 4. Altered recruitment of inflammatory cells into the lungs of PD-1$^{-/-}$ mice infected with *M. tuberculosis* H37Rv aerosol. (*A*) Lower numbers of CD4$^+$ T cells in the lungs of infected PD-1$^{-/-}$ mice at 4 wk postinfection. (*B*) CD8$^+$ T cell numbers are similar to control mice. (*C*) B cell numbers are reduced in the lungs of PD-1$^{-/-}$ mice at 4 wk postinfection ($P < 0.05$). Recruitment of myeloid cells such as macrophages (*D*, $P < 0.05$) and neutrophils (*E*) is increased in the lungs of PD-1$^{-/-}$ mice starting at 3 wk postinfection. Mice were infected with 135 CFU/mouse. FACS analysis was performed on total lung cells; data are shown as average ± SD of three mice per group at each timepoint.

different cytokine responses were likely to be present in the two different groups of infected mice. To test this hypothesis, the serum and lung lysate levels of multiple proinflammatory cytokines of infected wild-type and PD-1$^{-/-}$, as well as uninfected mice, were measured at different timepoints. Starting after 15 d and especially after 19 d postinfection there was a progressive increase in the levels of multiple proinflammatory cytokines in the sera of PD-1$^{-/-}$ mice. TNF-α and IL-1 were significantly increased by 28 d postinfection (Fig. 5 *A* and *B*). Most strikingly, at this timepoint the level of IL-6 was approximately sevenfold higher, whereas IL-17 was more than 40 times higher in infected PD-1$^{-/-}$ mice, compared with control mice (Fig. 5 *C* and *D*), indicating a substantially altered inflammatory response triggered by *M. tuberculosis* in the PD-1$^{-/-}$ mice. Notably, the serum levels of the effector cytokines IFN-γ and IL-12 were increased in the sera of PD-1$^{-/-}$ mice, despite of the higher bacterial load (Fig. 5 *E* and *F*). The level of the neutrophil chemoattractant and activating chemokine KC/GRO-α (CXCL1) was progressively increased in the PD-1$^{-/-}$ mice starting at day 19, consistent with the necrotic nature of the inflammation (Fig. 5*G*). IL-10 levels were not significantly different between PD-1$^{-/-}$ and wild-type mice at the timepoints examined (Fig. 5*H*). Uninfected animals had only low levels of serum cytokines, which were not significantly different in PD-1$^{-/-}$ and C57BL/6 mice, although a trend was observed toward higher values for TNF-α and IL-12p70 in some of the uninfected PD-1$^{-/-}$ mice.

The lung lysates of infected PD-1$^{-/-}$ mice also had higher levels of the proinflammatory cytokines IL-1 and IL-17 at 3 wk postinfection (Fig. 6 *A* and *B*). Chemokine KC/GRO-α was increased over 3.5-fold in the lungs of PD-1$^{-/-}$ mice (Fig. 6*C*). IL-10 was increased 1.5-fold, but this difference was not statistically significant (Fig. 6*D*). Notably, in contrast to the serum values, the effector cytokines IFN-γ and IL-12 were decreased in the lungs of PD-1$^{-/-}$ mice, compared with wild-type mice (Fig. 6 *E* and *F*) at 3 wk postinfection. Similarly, when total lung cells from infected mice were re-stimulated in vitro with H37Rv sonicate, the relative IFN-γ production was lower in the PD-1$^{-/-}$ lung cells, compared with cells from the control lungs (Fig. 6*G*).

Up-Regulated Inflammatory Gene Expression Profile in the Lungs of *M. tuberculosis*-Infected PD-1$^{-/-}$ Mice. To investigate the underlying physiological mechanism for the different susceptibility to *M. tuberculosis* infection in PD-1$^{-/-}$ versus wild-type C57BL/6 mice, and to characterize the profoundly different inflammation in the lungs, microarray experiments were performed. At 4 wk postinfection, by using high-stringency criteria for evaluation ($P < 0.05$, and changes of twofold or greater as cutoffs), 367 transcripts of genes were found to be differentially regulated in infected PD-1$^{-/-}$ versus wild-type lungs (Fig. S4*A*), 73% of which were increased and 27% decreased. A total of 230 of these differentially regulated transcripts correspond to genes that are known to function in various biological processes. Within this group of interest, 164 genes were up-regulated (71.3%) and 66 were down-regulated (28.7%) (Fig. S4*C*). The majority of the up-regulated genes are known to be involved in various aspects of immune responses (Fig. S4*D*). Notably, there was a marked increase in the level of chemokines that attract granulocytes, especially neutrophils (Table 1). In contrast, levels of chemokines and chemokine receptors attracting lymphocytes were decreased in the lungs of PD-1$^{-/-}$ mice (Table 1). These findings are consistent with the histopathology showing extensive neutrophilic infiltrates in the infected PD-1$^{-/-}$ lungs but no significant presence of lymphocytic infiltrates. In addition, the levels of several inflammatory cytokines were markedly increased in the PD-1$^{-/-}$ lungs, especially IL-1 and related molecules, and others such as TNF-α, IL-6, and IL-10 (Table 1). The genes that were significantly different were grouped on the basis of their functions (Tables S1 and S2). Changes in the gene expression levels correlated with cytokine measurements from the lung lysates and sera of infected mice (CXCL1, IL-1β, TNF-α, IL-6, and IL-10). Notably, only 16 genes had significantly different expression levels between uninfected PD-1$^{-/-}$ and wild-type mice, out of which only 6 have known biological function (Fig. S4*B* and Table S3).

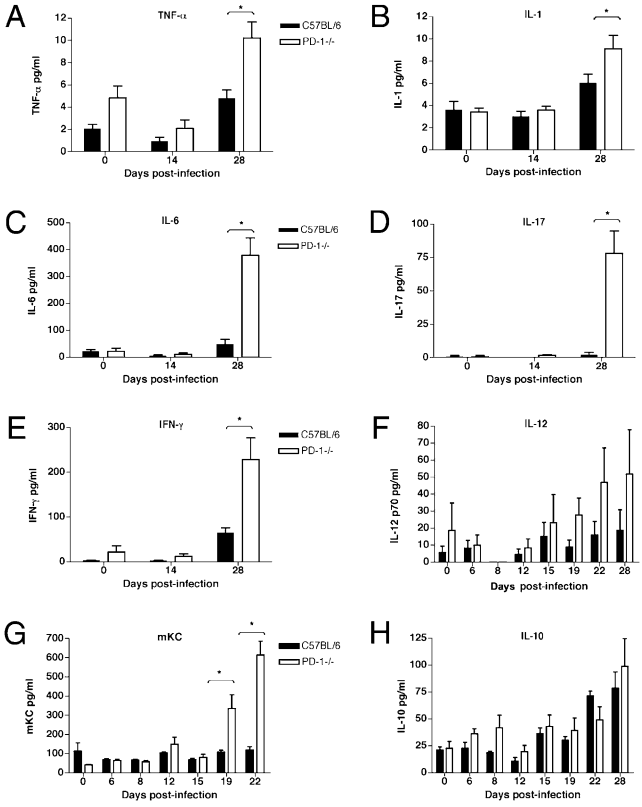

Fig. 5. Increased cytokine levels measured in the sera of PD-1$^{-/-}$ mice infected with low-dose *M. tuberculosis* aerosol. Proinflammatory cytokines TNF-α (*A*, $P < 0.001$), IL-1 (*B*, $P < 0.05$), and IL-6 (*C*, $P < 0.001$) were elevated in the sera of infected PD-1$^{-/-}$ mice at 4 wk postinfection. (*D*) Significantly increased IL-17 levels in infected PD-1$^{-/-}$ mice ($P < 0.001$). Higher levels of IFN-γ (*E*) and IL-12 (*F*) in the sera of infected PD-1$^{-/-}$ mice. (*G*) Chemokine KC (CXCL1) is selectively increased in infected PD-1$^{-/-}$ mice after 19 d ($P < 0.001$). (*H*) IL-10 levels are not significantly different between PD-1$^{-/-}$ and control mice. Mice were infected with H37Rv aerosol 50 CFU/mouse (*A–E*) or 135 CFU/mouse (*F–H*). Serum samples were analyzed from five mice at each timepoint; mean values are shown ± SD. *, statistical significance between groups.

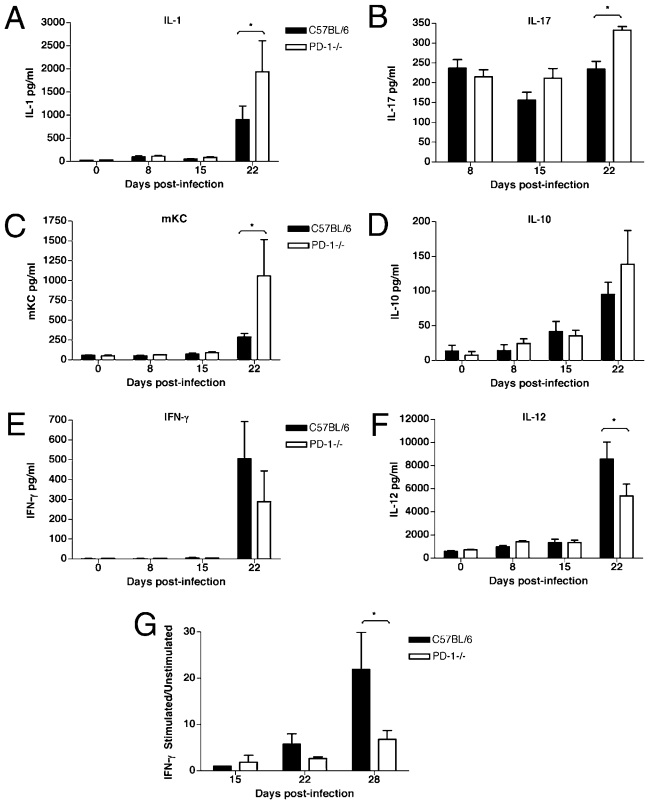

Fig. 6. Increased inflammatory and reduced effector cytokine levels in the lungs of PD-1$^{-/-}$ mice infected with *M. tuberculosis* aerosol. IL-1 (*A*, $P < 0.05$) and IL-17 (*B*, $P < 0.01$) are increased in the lungs of infected PD-1$^{-/-}$ mice at 3 wk postinfection. (*C*) Increased levels of chemokine KC (CXCL1) in PD-1$^{-/-}$ mice ($P < 0.05$). (*D*) Higher IL-10 levels in infected PD-1$^{-/-}$ lungs. Effector cytokine levels IFN-γ (*E*) and IL-12 (*F*, $P < 0.01$) are reduced in the lungs of PD-1$^{-/-}$ mice, compared with control mice at 3 wk postinfection. (*G*) Lung cells from infected PD-1$^{-/-}$ mice re-stimulated in vitro with H37Rv sonicate show less stimulation compared with C57BL/6 mice, measured by IFN-γ production ($P < 0.001$). Mice were infected with H37Rv aerosol 106 CFU/mouse (*A–F*), or 135 CFU/mouse (*G*). Data are shown as mean ± SD of four mice per group at each timepoint. *, statistical significance between groups.

Discussion

Although the importance of the PD-L/PD-1 pathway has been studied in various infection models, little is known about the role of this pathway in infection with *M. tuberculosis*. Of interest, one recent report showed that PD-1 is up-regulated on peripheral T cells of *M. tuberculosis*-infected patients and inhibits effector T cell functions such as IFN-γ production and lytic degranulation of CD8$^+$ T cells in vitro. Blockade of PD-1 in this system enhanced effector functions of T cells (13). Because blockade of the inhibitory receptor PD-1 serves as a promising therapeutic tool in various infection models, including our earlier studies on *H. capsulatum* (12), we hypothesized that mice that lack PD-1 would mount a more efficient immune response against *M. tuberculosis* and possibly show enhanced bacterial clearance.

Surprisingly and paradoxically, PD-1–deficient mice showed extreme sensitivity to *M. tuberculosis*, succumbing as early as 39 d after medium-dose aerosol infection (320 CFU/mouse) and showing massive bacterial proliferation in the lungs. The lower survival rate and higher pathogen burden of the PD-1$^{-/-}$ mice compared with control mice was striking and unexpected, given the fact that PD-1 is an immune inhibitory receptor that has been shown to attenuate T and B cell activation and has an important role in peripheral immune tolerance (5–6, 14). Consistent with these findings, PD-1 deficiency in mice is known to trigger susceptibility to various autoimmune diseases, depending on the genetic background (15). PD-1$^{-/-}$ mice in the C57BL/6 background used here develop lupus-like arthritis and glomerulonephritis at over 6 mo of age (16). However, studies of these mice at younger ages have not shown any gross immunological alterations other than moderate splenomegaly with increased cellularity (17). To assess whether persistent infection could have an effect on the development of autoimmunity, we followed serum creatinine and blood urea nitrogen values after *M. tuberculosis* aerosol infection. This showed no significant difference between infected and noninfected PD-1$^{-/-}$ mice (data not shown), suggesting that the observed severity of the infection was unlikely to be due to enhanced autoimmunity triggered by the infection.

In addition to the shortened survival and higher CFU counts, lungs of the PD-1$^{-/-}$ mice developed extremely severe multifocal necrotic pneumonia that was strikingly different in its extent and character from the inflammation caused in wild-type mice. PD-1$^{-/-}$ mice developed extensive necrotic nodules with clusters of degenerating neutrophils and macrophages, but no significant lymphocytic infiltrates. The observed character of the necrotic lung lesions in the absence of PD-1 was reminiscent of those induced by mycobacterial infection in mice that are deficient in TNF-α (2) or in MyD88 (18). There is evidence that both of these molecules are crucial regulators of first-line innate responses to *M. tuberculosis*, which raises the issue of whether the PD-1/PD-L pathway might

Table 1. Differential gene expression levels of chemokines and proinflammatory cytokines in the lungs of infected PD-1$^{-/-}$ mice, compared with control mice

Gene	Fold change (log 2)	Description	GeneBank accession no.
Chemokines			
Cxcl2	3.91	Chemokine (CXC) ligand 2	NM_009140
Ccl3	2.90	Chemokine (CC) ligand 3	NM_011337
Il8rb	2.55	Interleukin 8 receptor, beta	NM_009909
Ccr1	2.41	Chemokine (CC) receptor 1	NM_009912
Ccl4	2.39	Chemokine (CC) ligand 4	NM_013652
Cxcl5	1.55	Chemokine (CXC) ligand 5	NM_009141
Cxcl1	1.12	Chemokine (CXC) ligand 1	NM_008176
Ccrl2	1.10	Chemokine (CC) receptor-like 2	NM_017466
Cxcl13	1.08	Chemokine (CXC) ligand 13	NM_018866
Ccl21a	−1.22	Chemokine (CC) ligand 21a	NM_011335
Xcr1	−1.32	Chemokine (C) receptor 1	NM_011798
Proinflammatory cytokines			
Il1f9	4.00	Interleukin 1 family, member 9	NM_153511
Il1r2	3.18	Interleukin 1 receptor, type II	NM_010555
Il1a	2.76	Interleukin 1 alpha	NM_010554
Il6	2.41	Interleukin 6	NM_031168
Il1rn	2.27	Interleukin 1 receptor antagonist, transcript variant 1	NM_031167
Il1b	2.09	Interleukin 1 beta	NM_008361
Tnf	1.42	Tumor necrosis factor	NM_013693
Il1rap	1.17	Interleukin 1 receptor accessory protein, transcript variant 1	NM_008364
Il10	1.04	Interleukin 10	NM_010548

also have a role in regulating early innate and inflammatory responses after infection.

Study of the kinetics of cell recruitment to the lungs after *M. tuberculosis* infection showed early recruitment of macrophages and neutrophils into the lung infiltrates of infected PD-1$^{-/-}$ mice. The fewer number of B cells and CD4^{+} T cells compared with control mice could negatively impact the adaptive immune response in the lungs of PD-1$^{-/-}$ mice, which is consistent with their inability to control bacterial proliferation, as demonstrated by the 10-fold higher bacterial loads in the lungs.

Consistent with the striking differences in pathology and cellular recruitment, cytokine responses were also significantly different between infected PD-1$^{-/-}$ and wild-type mice. PD-1$^{-/-}$ mice had significantly higher levels of the serum proinflammatory cytokines TNF-α and IL-1β. Although TNF-α is an essential effector cytokine involved in controlling tuberculosis, increased TNF-α levels can be associated with tissue damage, and TNF-α gene expression is increased at higher levels in infected mouse strains that are susceptible to tuberculosis (19). In addition, the levels of IL-6 and IL-17 were much higher in both the sera and lungs of infected PD-1$^{-/-}$ mice, compared with control mice. It has been shown that protective immunity to tuberculosis, along with a Th1 response, requires IL-17-producing T_H17 and γδ-T cells that attract neutrophils (20). IL-17 has also been implicated as an important mechanism for the maintenance of the inflammatory response and for the development of the Th1 response required for protective immunity in tuberculosis (21). However, excessive IL-17 levels can lead to exacerbated inflammation, with increased neutrophil recruitment and tissue damage. In addition, increased level of the neutrophil attracting chemokine CXCL1 (KC) in both the sera and lungs of infected PD-1$^{-/-}$ mice further contributed to the increased number of neutrophils observed. Interestingly, although the effector cytokines IL-12 and IFN-γ were increased in the sera of infected PD-1$^{-/-}$ mice, they showed significantly lower levels in the lungs compared with the control mice. In addition, restimulation of total lung cells with H37Rv sonicate also resulted in reduced stimulation in the PD-1$^{-/-}$ mice, as shown by their lower relative IFN-γ production. This could be due to the reduced number of T cells present in the lungs or their insufficient activation within the aberrant inflammatory milieu in the lungs. However, lower IFN-γ levels in the lung have a negative impact on macrophage functions, such as elimination of bacteria after phagocytosis, which could explain why bacterial loads were increasing in the lungs of PD-1$^{-/-}$ mice.

Consistent with the severe lung phenotype of the infected PD-1$^{-/-}$ mice, microarray analysis showed significantly up-regulated inflammatory gene expression profile in the lungs of PD-1$^{-/-}$ mice, compared with infected control mice. More than 70% of the differentially expressed genes were up-regulated in the PD-1$^{-/-}$ mice, the majority of which are involved in immune responses against pathogens. Notably, the expression of multiple chemokines that attract neutrophils was increased, whereas expression of chemokines and chemokine receptors involved in lymphocyte recruitment was decreased (Table 1). These findings help to explain the observed necrotic character of the inflammation in the lungs of the PD-1$^{-/-}$ mice. Furthermore, multiple proinflammatory cytokines were up-regulated in the PD-1$^{-/-}$ lungs, primarily members of the IL-1 family, as well as other cytokines including TNF-α, IL-6, and IL-10 (Table 1). The up-regulation of multiple genes involved in inflammatory processes detected by microarray was consistent with the observed severe necrotic inflammation in the lungs of PD-1$^{-/-}$ mice, and with the observed up-regulated proinflammatory cytokine pattern detected in the lungs and sera.

In summary, these data show that there is a substantially increased inflammatory and necrotic response to *M. tuberculosis* in the absence of PD-1, indicating an essential role for this co-inhibitory receptor in controlling inflammatory responses to a highly immunogenic pathogen. In contrast to the results obtained in chronic viral infection models, where blockade of PD-1 induced increased effector functions in T cells, and more robust response against the pathogen, *M. tuberculosis* infection is fatal when the PD-1 pathway is rendered nonfunctional by gene deletion. Pathogen-related differences in PD-1 regulation have recently been indicated by a study showing that PD-L1 blockade suppressed antibacterial protection in

infection with *Listeria monocytogenes*, suggesting a protective role for PD-L1 in antibacterial immunity (22, 23). In addition, although PD-1 has been known to primarily regulate adaptive immune responses, such as T and B cell activation, two recent studies suggest that it could also regulate innate responses to bacterial infections. One study found that PD-1 expressed on splenic dendritic cells under inflammatory conditions negatively regulated dendritic cell functions during innate immune response against *Listeria* (24). Another study reported that PD-1 was up-regulated on peritoneal macrophages in sepsis, inhibiting the innate inflammatory response (25). However, in both of these models PD-1$^{-/-}$ mice were more resistant to the disease than wild-type mice, suggesting a unique role for PD-1 in regulating the pathogenesis of tuberculosis.

Overall, our studies extend the role of the PD-L/PD-1 pathway in regulating antimicrobial immunity to *M. tuberculosis* infection and show that the presence of this pathway is essential to control fatal inflammatory responses in the lung after *M. tuberculosis* aerosol. These findings could have relevance to immunotherapeutic approaches targeting the PD-1 pathway in other infection models (e.g., chronic viral infections), which should be considered cautiously in cases of co-infection with *M. tuberculosis*.

Materials and Methods

Mice. C57BL/6 mice (6–12 wk old) were purchased from Jackson Laboratories. PD-1$^{-/-}$ mice on the C57BL/6 background were kindly provided by Tasuku Honjo (Kyoto University, Kyoto, Japan). Mice were backcrossed for more than 10 generations and used in the experiments at 6–12 wk of age. All mice were maintained in pathogen-free conditions in the animal facility at Albert Einstein College of Medicine (AECOM). All animal work was approved and performed according to the guidelines set by the AECOM Institutional Animal Care and Use Committee.

Bacterial Strains and Aerosol Challenge. The virulent *M. tuberculosis* H37Rv strain was obtained from Trudeau Institute. Cell growth conditions, aerogenic challenge, and determination of CFU counts in tissues are described in *SI Materials and Methods*.

Histology and Immunohistochemistry. Histological analysis is described in detail in *SI Materials and Methods*.

FACS Analysis. Single-cell suspensions from lungs were prepared and FACS staining was performed as described in *SI Materials and Methods*.

Cytokine Measurements. Cytokines from sera and lung lysates were measured using Mouse Proinflammatory 7-plex kit (Meso Scale Discovery), as described in *SI Materials and Methods*. IL-17 was measured using ELISA kits from Quantikine (R&D Systems) and eBiosciences.

RNA Extraction and Microarray Experiments. Lungs from PD-1$^{-/-}$ and C57BL/6 mice infected with *M. tuberculosis* H37Rv (173 CFU per lung), as well as from uninfected mice were used for total RNA extraction and microarray experiments, using GeneChip Mouse Gene 1.0 ST Arrays (Affymetrix), as described in *SI Materials and Methods*. The microarray data were analyzed as described in *SI Materials and Methods*.

Statistical Analysis. Statistical analysis was performed using Prism4 GraphPad software. Survival curves on Fig. 1 were compared by log rank test. To compare multiple groups in Figs. 2 and 4–6, one-way ANOVA was used, followed by Bonferroni's multiple comparison test. Statistical significance was defined as a P value of <0.05.

ACKNOWLEDGMENTS. We thank Tasuku Honjo (Kyoto University, Kyoto, Japan) and Lieping Chen (The Johns Hopkins University, Baltimore, Maryland) for providing the PD-1$^{-/-}$ mice. We thank Brian Weinrick for technical help, Michael Goldberg for providing the H37Rv sonicate, and John Kim and Mei Chen for help with the animal work. We thank the Histopathology Shared Resource of the Albert Einstein Cancer Center, especially Rani Sellers, for help with the histological analysis; the Affymetrix Gene Chip Facility; and the Flow Cytometry Core Facilities of the Albert Einstein Cancer Center (P30CA-013330) and Center for AIDS Research [National Institutes of Health (NIH) AI-51519]. S.C.A. and S.G.N. are supported by NIH Grant AI-07289. W.R. J. and S.A.P. are supported by NIH Program Project AI-063537. W.R.J. is supported by NIH Grant AI-2617O and also in part by the Center for AIDS Research at the Albert Einstein College of Medicine and Montefiore Medical Center funded by NIH Grant AI-51519.

1. McShane H (2005) Co-infection with HIV and TB: Double trouble. *Int J STD AIDS* 16: 95–100, quiz 101.
2. Flynn JL, et al. (1995) Tumor necrosis factor-alpha is required in the protective immune response against Mycobacterium tuberculosis in mice. *Immunity* 2:561–572.
3. Flynn JL, Chan J (2001) Immunology of tuberculosis. *Annu Rev Immunol* 19:93–129.
4. Greenwald RJ, Freeman GJ, Sharpe AH (2005) The B7 family revisited. *Annu Rev Immunol* 23:515–548.
5. Freeman GJ, et al. (2000) Engagement of the PD-1 immunoinhibitory receptor by a novel B7 family member leads to negative regulation of lymphocyte activation. *J Exp Med* 192:1027–1034.
6. Latchman Y, et al. (2001) PD-L2 is a second ligand for PD-1 and inhibits T cell activation. *Nat Immunol* 2:261–268.
7. Sharpe AH, Wherry EJ, Ahmed R, Freeman GJ (2007) The function of programmed cell death 1 and its ligands in regulating autoimmunity and infection. *Nat Immunol* 8:239–245.
8. Barber DL, et al. (2006) Restoring function in exhausted CD8 T cells during chronic viral infection. *Nature* 439:682–687.
9. Day CL, et al. (2006) PD-1 expression on HIV-specific T cells is associated with T-cell exhaustion and disease progression. *Nature* 443:350–354.
10. Smith P, et al. (2004) Schistosoma mansoni worms induce anergy of T cells via selective up-regulation of programmed death ligand 1 on macrophages. *J Immunol* 173:1240–1248.
11. Terrazas LI, Montero D, Terrazas CA, Reyes JL, Rodríguez-Sosa M (2005) Role of the programmed Death-1 pathway in the suppressive activity of alternatively activated macrophages in experimental cysticercosis. *Int J Parasitol* 35:1349–1358.
12. Lázár-Molnár E, et al. (2008) The PD-1/PD-L costimulatory pathway critically affects host resistance to the pathogenic fungus *Histoplasma capsulatum*. *Proc Natl Acad Sci USA* 105:2658–2663.
13. Jurado JO, et al. (2008) Programmed death (PD)-1:PD-ligand 1/PD-ligand 2 pathway inhibits T cell effector functions during human tuberculosis. *J Immunol* 181:116–125.
14. Okazaki T, Maeda A, Nishimura H, Kurosaki T, Honjo T (2001) PD-1 immunoreceptor inhibits B cell receptor-mediated signaling by recruiting src homology 2-domain-containing tyrosine phosphatase 2 to phosphotyrosine. *Proc Natl Acad Sci USA* 98:13866–13871.
15. Okazaki T, Honjo T (2006) The PD-1-PD-L pathway in immunological tolerance. *Trends Immunol* 27:195–201.
16. Nishimura H, Nose M, Hiai H, Minato N, Honjo T (1999) Development of lupus-like autoimmune diseases by disruption of the PD-1 gene encoding an ITIM motif-carrying immunoreceptor. *Immunity* 11:141–151.
17. Nishimura H, Minato N, Nakano T, Honjo T (1998) Immunological studies on PD-1 deficient mice: Implication of PD-1 as a negative regulator for B cell responses. *Int Immunol* 10:1563–1572.
18. Fremond CM, et al. (2004) Fatal Mycobacterium tuberculosis infection despite adaptive immune response in the absence of MyD88. *J Clin Invest* 114:1790–1799.
19. Keller C, et al. (2006) Genetically determined susceptibility to tuberculosis in mice causally involves accelerated and enhanced recruitment of granulocytes. *Infect Immun* 74:4295–4309.
20. Korbel DS, Schneider BE, Schaible UE (2008) Innate immunity in tuberculosis: Myths and truth. *Microbes Infect* 10:995–1004.
21. Khader SA, et al. (2007) IL-23 and IL-17 in the establishment of protective pulmonary CD4+ T cell responses after vaccination and during Mycobacterium tuberculosis challenge. *Nat Immunol* 8:369–377.
22. Rowe JH, Johanns TM, Ertelt JM, Way SS (2008) PDL-1 blockade impedes T cell expansion and protective immunity primed by attenuated Listeria monocytogenes. *J Immunol* 180:7553–7557.
23. Seo SK, et al. (2008) Blockade of endogenous B7-H1 suppresses antibacterial protection after primary Listeria monocytogenes infection. *Immunology* 123:90–99.
24. Yao S, et al. (2009) PD-1 on dendritic cells impedes innate immunity against bacterial infection. *Blood* 113:5811–5818.
25. Huang X, et al. (2009) PD-1 expression by macrophages plays a pathologic role in altering microbial clearance and the innate inflammatory response to sepsis. *Proc Natl Acad Sci USA* 106:6303–6308.